

Arsenic trioxide induces ROS activity and DNA damage, leading to G0/G1 extension in skin fibroblasts through the ATM-ATR-associated Chk pathway

Jutapon Chayapong¹ · Harishkumar Madhyastha¹  · Radha Madhyastha¹ · Queen Intan Nurrahmah¹ · Yuichi Nakajima¹ · Narantsog Choijookhuu² · Yoshitaka Hishikawa² · Masugi Maruyama¹

Received: 16 February 2016 / Accepted: 6 December 2016 / Published online: 24 December 2016
© Springer-Verlag Berlin Heidelberg 2016

Abstract Arsenic (As) toxicity is a global health problem, affecting millions of people. Exposure to arsenic, mostly via drinking water, has been associated with cancer of skin, lungs, and blood, in addition to several kinds of skin lesions. The present study focused on the effect of arsenic trioxide (As₂O₃) on normal skin fibroblast cells. Specifically, the effect of As₂O₃ on ROS generation and oxidative stress was investigated. Proteins involved in the DNA damage signaling pathway and cell cycle were also studied. As₂O₃ induced the generation of intracellular ROS. Immunohistochemistry analysis revealed a dose-dependent increase in the number of 8-OHdG-positive cells, an indication of oxidative stress. Cell cycle analysis by flow cytometry demonstrated that As₂O₃ caused a significant percentage of cells to accumulate in the G0/G1 phase with a concomitant reduction in the S phase. Increases in the activated forms of DNA damage signaling proteins, ATM and ATR, and their effector molecules, Chk2 and p53, were also observed. In addition, expression of oncogene p21 was also increased. The study shows that exposure of normal skin fibroblast cells to As₂O₃ could lead to cell cycle arrest through ATM/ATR and DNA damage signaling pathways. In conclusion, we report here that arsenic trioxide increases cellular oxidative stress leading to shift in cell cycle and leads to DNA damage through ATM/ATR and the CHK-dependent signaling pathway.

Keywords Arsenic trioxide · DNA damage · G0/G1 · Cell cycle arrest

Introduction

Arsenic is a naturally occurring element, widely distributed in the environment and deposited in the earth's crust as a metalloid. Arsenic occurs in either trivalent or pentavalent form of oxidative state; the trivalent (arsenic tri-oxide, As₂O₃) form is more toxic than the pentavalent form (Yu et al. 2006). Arsenic toxicity is a global health problem, affecting millions of people. It is estimated that over 100 million people worldwide are exposed to carcinogenic levels of arsenic (IARC 2004), with significant exposures identified in Bangladesh, India, Taiwan, China, Mexico, Argentina, Chile, Europe, and regions of North America (Reichard and Puga 2010). Exposure to arsenic has been associated with cancer of skin, lungs, and blood, in addition to several kinds of skin lesions such as hyperpigmentation, hyperkeratosis, and gangrene (Chen et al. 1992; Smith and Smith 2004; WHO 2006). It is classified as a group I human carcinogen by the International Agency for Research on Cancer (IARC 2004). Arsenic toxicity and subsequent generation of cellular reactive oxygen species (ROS) during arsenic metabolism can play an important role in arsenic cellular toxicity. Oxidative stress is proposed as a potential mode of carcinogenic action of As₂O₃ (Ding et al. 2005). Arsenic causes oxidative stress by triggering generation of intracellular ROS (Ding et al. 2005). Oxidative stress can then elicit DNA damage (Dilda and Hogg 2007) and induce cellular senescence (Yamaguchi et al. 2016) or apoptosis (You and Park 2012).

The first signs of chronic exposure to arsenic include skin pigmentation/depigmentation, hyperkeratosis of palms and

Responsible editor: Markus Hecker

✉ Masugi Maruyama
masugi@med.miyazaki-u.ac.jp

¹ Department of Applied Physiology, Faculty of Medicine, University of Miyazaki, Miyazaki 889-1692, Japan

² Department of Anatomy, Histochemistry and Cell Biology, Faculty of Medicine, University of Miyazaki, Miyazaki 889-1692, Japan

soles, and skin lesions. Physiologically speaking, skin is a dynamic organ, encompassing a complex network of various cell types and functioning as the first barrier of protection from environmental damage. Fibroblast cells form a major component of the skin and play a crucial role in regulating skin physiology. They help in establishing skin structure and function through production and assembly of extracellular matrix and interaction with other cell types. They are model cells for studies on wound and other skin pathologies (Madhyastha et al. 2010). To our knowledge, information about the effect of arsenic on skin fibroblasts is scarce (Graham-Evans et al. 2003). Hence, this study was undertaken to investigate the effect of As₂O₃ on normal skin fibroblasts. The consequences on cell cycle progression and DNA damage were also studied, using mouse skin fibroblast cells. The findings showed that As₂O₃ induced cell cycle arrest through ATM/ATR and DNA damage signaling pathways, and that it caused overexpression of the oncogene p21.

Materials and methods

Chemicals

As₂O₃ was purchased from Kanto Chemical Co., (Tokyo, Japan). Stock solution of 1 M As₂O₃ was prepared by dissolving the powder in water. Alpha-Minimum Essential Medium (α -MEM) was purchased from Sigma Chemicals (St. Louis, MO, USA). Fetal bovine serum (FBS) and antibiotic mixture (5 mg/ml of penicillin, 5 mg/ml of streptomycin, and 10 mg/mL neomycin) (PSN) were purchased from Gibco (Tokyo, Japan). 3-(4,5-Dimethylthiazol2-yl)-2,5-diphenyl tetrazolium bromide (MTT) reagent was purchased from Nacalai Tesque Ltd. (Osaka, Japan). Biotin-16-dUTP and terminal deoxynucleotidyl transferase (TdT) were purchased from Roche (Mannheim, Germany). 3,3'-Diaminobenzidine/4HCl and Brij L23 were purchased from Dojin Laboratories (Tokyo, Japan) and Sigma Chemical (St. Louis, MO, USA), respectively. All other reagents were purchased from Wako Pure Chemical Industries Ltd. (Osaka, Japan).

Cell culture

Mouse skin fibroblast cells, m5S, were purchased from the RIKEN Cell Bank (Tsukuba, Japan). Cells were cultured in α -MEM supplemented with 10% (v/v) heat-inactivated FBS and 1% (v/v) PSN at a humidified chamber (5% CO₂, 37 °C). Cells from passages 2–5 were used in the experiments. At the semi-confluent stage, cells were incubated with different concentrations of As₂O₃ (0 to 500 μ M) in serum-free conditions, for 18 h, and analyzed for different parameters.

Cytotoxicity assay

Cytotoxicity was determined by LDH assay, using CytoTox 96® Non-Radioactive Cytotoxicity Assay Kit (Promega, Madison, WI, USA). Cells, seeded in 96-well plates at a density of 1×10^4 cells/well, were treated with different concentrations of As₂O₃ (0, 10, 50, 100, 500 μ M) under serum-free conditions, for 18 h. Cells (3rd passage) were maintained at 37 °C in a saturated humidity atmosphere containing 95% air and 5% CO₂ with 1% antibiotic anti-mycotic solution (1000 U/ml penicillin G, 10 mg/ml streptomycin sulfate, 5 mg/ml gentamicin, and 25 μ g/ml amphotericin B). Supernatants were collected to determine the amount of lactate dehydrogenase released as a result of cytotoxicity. The amount of enzyme released was quantified using a Multiskan FC spectrophotometer (Thermo Fisher Scientific Inc., Pittsburgh PA, USA) at an absorbance of 490 nm. Data from three independent experiments, each performed in triplicate, was analyzed for cytotoxicity effect.

Cell viability assay

Cells were seeded in 96-well plates at a density of 1×10^4 cells/well and treated with different concentrations of As₂O₃ (0, 10, 50, 100, 500 μ M) in serum-free conditions for 18 h. Cells were maintained at 37 °C in a saturated humidity atmosphere containing 95% air and 5% CO₂ with 1% antibiotic anti-mycotic solution (1000 U/ml penicillin G, 10 mg/ml streptomycin sulfate, 5 mg/ml gentamicin, and 25 μ g/ml amphotericin B). The effect on viability was determined by MTT assay, following standard procedures (Mosmann 1983). Intracellular formazan was used to determine cell viability and was quantified with a Multiskan FC spectrophotometer, at an absorbance of 570 nm. Data from three independent experiments, each performed in triplicate, was analyzed for effect of As₂O₃ on cell viability.

Quantification of intracellular reactive oxygen species assay

Intracellular ROS was quantified using OxiSelect™ Intracellular ROS Assay Kit (Cell Biolabs, Inc., San Diego CA, USA). For this assay, cells were seeded in 96-well plates at a density of 1×10^4 cells/well. Cells were maintained at 37 °C in a saturated humidity atmosphere containing 95% air and 5% CO₂ with 1% antibiotic anti-mycotic solution (1000 U/ml penicillin G, 10 mg/ml streptomycin sulfate, 5 mg/ml gentamicin, and 25 μ g/ml amphotericin B). Following 18 h of incubation with various doses of As₂O₃ (0, 10, 50, 100, 500 μ M) under serum-free conditions, cells were washed with Hank's Balanced Salt Solution. Dichlorofluorescein diacetate (DCFH-DA) was added to the cells at 37 °C for 1 h in the dark. Non-fluorescent DCFH-DA

is converted to fluorescent DCF in proportion to the amount of ROS generation in cells (Crow 1997). The fluorescence signals were quantified by spectrofluorometry using a DTX 800 spectrofluorometer (Beckman, Pasadena CA, USA) at excitation and emission wavelengths of 485 and 530 nm, respectively. Results were expressed as arsenic concentration vs relative fluorescence intensity. Data shown is a representative of three independent experiments; each experiment was performed in triplicate.

Intracellular ROS detection by fluorescence microscopy

Intracellular ROS was also detected by fluorescence microscopy using OxiSelect™ Intracellular ROS Assay Kit (Cell Biolabs, Inc.). Cells were seeded on coverslips in six-well plates at a density of 3×10^5 cells/well. Cells were maintained at 37 °C in a saturated humidity atmosphere containing 95% air and 5% CO₂ with 1% antibiotic anti-mycotic solution (1000 U/ml penicillin G, 10 mg/ml streptomycin sulfate, 5 mg/ml gentamicin, and 25 µg/ml amphotericin B). Following 18 h of incubation with 100 µM As₂O₃ under serum-free condition, cells were washed with PBS, and 10 µM DCFH-DA was added to cells at 37 °C for 1 h in the dark. Coverslips were mounted and images captured at $\times 10$ objective power, using a fluorescence microscope (Keyence BZ-9000, Osaka, Japan) at excitation and emission wavelengths of 485 and 530 nm, respectively. Images were obtained from 10 random fields per condition. A total of nine slides per condition from three independent experiments were counted.

Immunostaining for 8-OHdG

The effect of As₂O₃ on oxidative stress was analyzed by employing 8-hydroxydeoxyguanosine (8-OHdG). 8-OHdG is a standard cellular marker employed to study oxidative stress and assess DNA damage (Halliwell 2000). Cells were seeded on coverslips in six-well plates at a density of 3×10^5 cells/well. Following 18 h of standard cell culture condition incubation of cells with different concentrations of As₂O₃ (0, 100, 500 µM) under serum-free conditions, cells were washed with PBS and fixed with 4% paraformaldehyde in PBS for 10 min at room temperature. Cellular endogenous peroxidase activity was blocked with 0.3% H₂O₂ in absolute methanol for 15 min at room temperature and washed with PBS. Non-specific binding sites were blocked by 1 h of incubation at room temperature with 0.5 mg/ml normal goat IgG and 1% bovine serum albumin (BSA) in PBS. Cells were incubated with anti-8-OHdG anti-mouse monoclonal antibody (Nikken SEIL Co. Ltd., Tokyo, Japan) for 2 h at room temperature. The cells were washed three times with PBS containing 0.075% Brij® 35 and incubated with HRP-conjugated goat anti-mouse IgG (Cell Signaling Co. Ltd.,

Washington, USA) for 1 h at room temperature. After washing with 0.075% Brij® 35 in PBS, cells were stained with DAB and H₂O₂ in the presence of nickel and cobalt ions in the dark. Finally, coverslips were mounted and images captured using an Olympus microscope (BX53 Olympus, Tokyo, Japan) coupled to a digital camera at $\times 20$ magnification. Positively stained cells (dark color) from 20 visual fields were counted at random by three independent cytologists and graph plotted as the number of positive cells vs As₂O₃ concentration. A total of nine slides per condition from three independent experiments were counted.

Western blotting

Cells were seeded in six-well plates at a density of 3×10^5 cells/well under standard cell culture condition. Following incubation of cells with various doses of As₂O₃ (0, 25, 75, 100, 200, 500 µM) under serum-free conditions for 18 h, total cell lysates were prepared using radioimmunoprecipitation (RIPA) buffer. Protein fractions were resuspended in sodium dodecyl sulfate-polyacrylamide gel electrophoresis (SDS-PAGE) buffer containing 2-mercaptoethanol and boiled at 95 °C for 5 min. Protein samples were subjected to SDS-PAGE in 10% polyacrylamide gel and subsequently electroblotted onto polyvinylidene difluoride membranes (GE Healthcare, Piscataway Township, NJ, USA). After blocking non-specific binding sites for 1 h in 3% non-fat milk in TBST (TBS and 0.1% Tween 20), membranes were incubated overnight at 4 °C with primary antibodies specific for Chk1, Chk2, p53, pATM, pATR, p21, and H₂AX (Cell Signaling Inc., Beverly, MA, USA). The membranes were washed in TBST and incubated further with horseradish peroxidase-conjugated secondary antibodies at room temperature. Protein bands were detected using an enhanced ECL kit (GE Healthcare, Tokyo, Japan) with the digital imaging system (LAS4000, Fujifilm, Tokyo, Japan). Bands were measured using ImageQuant TL software (GE Healthcare Life Sciences). Data shown is a representative of three independent experiments; each experiment was performed in triplicate.

Terminal dUTP nick end-labeling staining

Terminal dUTP nick end-labeling (TUNEL) assay was carried out according to the method of Gavrieli et al. (1992) with a slight modification, as described previously (Hishikawa et al. 2004). Cells were seeded on coverslips in six-well plates at a density of 3×10^5 cells/well and treated with 100 µM As₂O₃ in serum-free conditions for 18 h. Treated cells were fixed with 4% paraformaldehyde in phosphate-buffered saline (PBS) for 15 min and washed with PBS. Cells were incubated with 1× TdT buffer (25 mM Tris-HCl buffer, pH 6.6, containing 0.2 M potassium cacodylate and 0.25 mg/ml

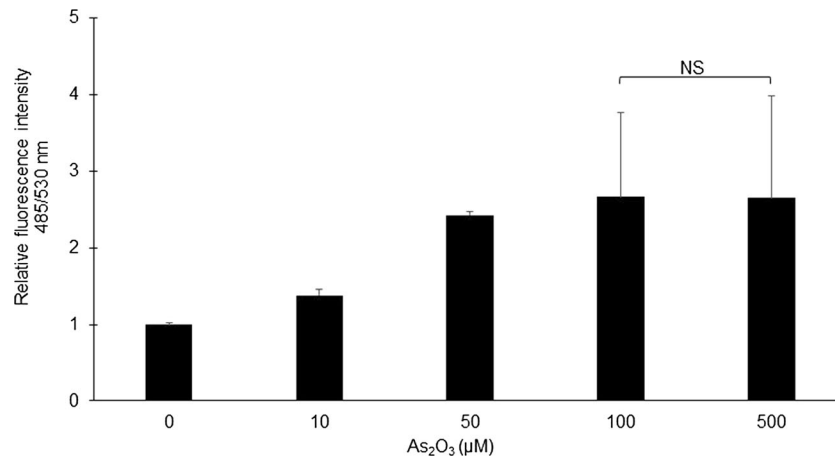


Fig. 1 Intracellular ROS release assay. Mouse skin fibroblast cells were treated with different concentrations of As₂O₃ (0, 10, 50, 100, 500 μM) in serum-free conditions, for 18 h. Intracellular ROS production was measured by using ROS assay kit. Representative graphs were plotted as relative fluorescence intensity 485/530 nm against different

concentrations of As₂O₃. Values are presented as mean ± SEM from three independent experiments. Non-significant (NS) groups were marked. Non-marked groups showed significant (*p* < 0.05) difference as analyzed by the Kruskal-Wallis test

BSA) for 30 min at RT. After incubation, cells were reacted with 800 units/ml TdT dissolved in TdT buffer supplemented with 1.5 mM CoCl₂, 0.5 μM biotin-16-dUTP, 20 μM dATP, and 0.1 mM dithiothreitol for 90 min at 37 °C. The reaction was terminated by washing with 50 mM Tris-HCl buffer (pH 7.4), and endogenous peroxidase activity was inhibited by immersing the slides in 0.3% H₂O₂ in methanol for 15 min at RT followed by washing with PBS. After incubation with 500 μg/ml normal goat IgG in 5% BSA in PBS for 60 min at

RT, the cells were incubated with HRP goat anti-biotin antibody (1:100) diluted with 5% BSA in PBS for 60 min at RT. After washing with 0.075% of Brij L23 in PBS, cells were stained with DAB and H₂O₂ in the presence of nickel and cobalt ions in the dark. Finally, coverslips were mounted and images captured using Olympus microscope (BX53 Olympus, Tokyo, Japan) coupled to a digital camera at ×20 objective. Positive cells from 20 visual fields were counted at random by three independent cytologists and graph plotted as the number

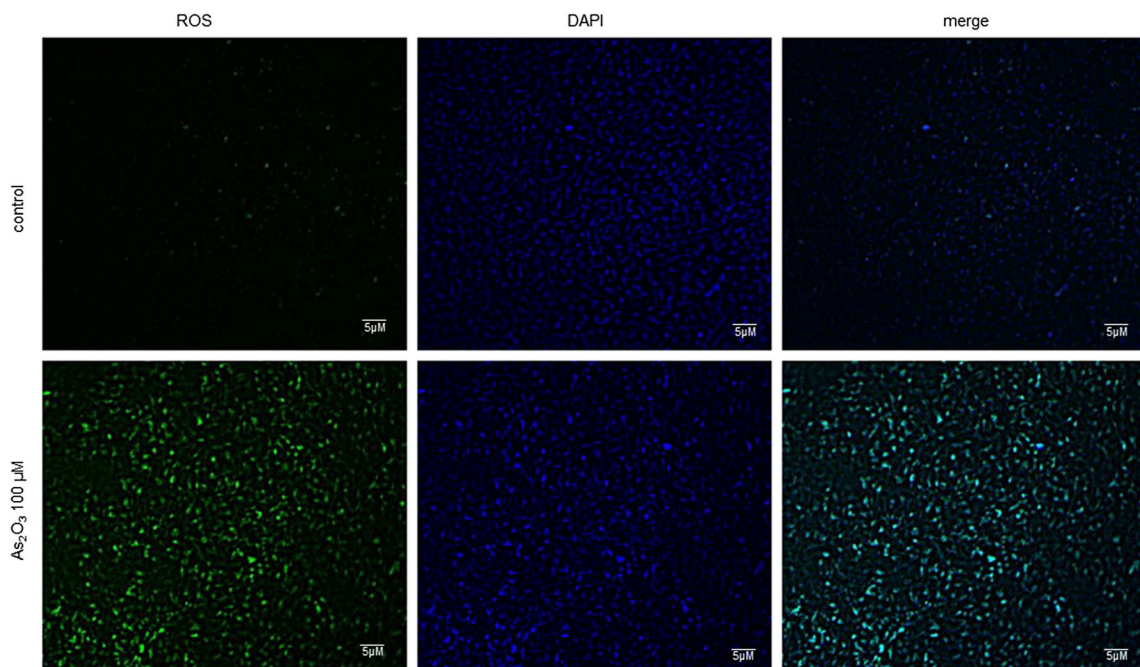


Fig. 2 Intracellular cellular ROS expression assay. Intracellular ROS accumulation following stimulation with 100 μM As₂O₃ was measured by fluorescent microscopy (×10). Cells fluorescing in green indicated

intracellular ROS production. Non-treated groups showed non-fluorescence. Nuclear stains were done with DAPI (blue color)

Fig. 3 Intracellular oxidative stress assay by immunocytochemistry of 8-OHdG. Fibroblast cells were treated with different concentrations of As_2O_3 (0, 100, and 500 μM) and were processed for 8-OHdG by immunocytochemical methods. Cells treated with 500 μM As_2O_3 expressed more number of positive cells (*black arrow*). *Bar graph* represents number of positive cells in 20 random high-power fields. Values are presented as mean \pm SEM from three independent experiments

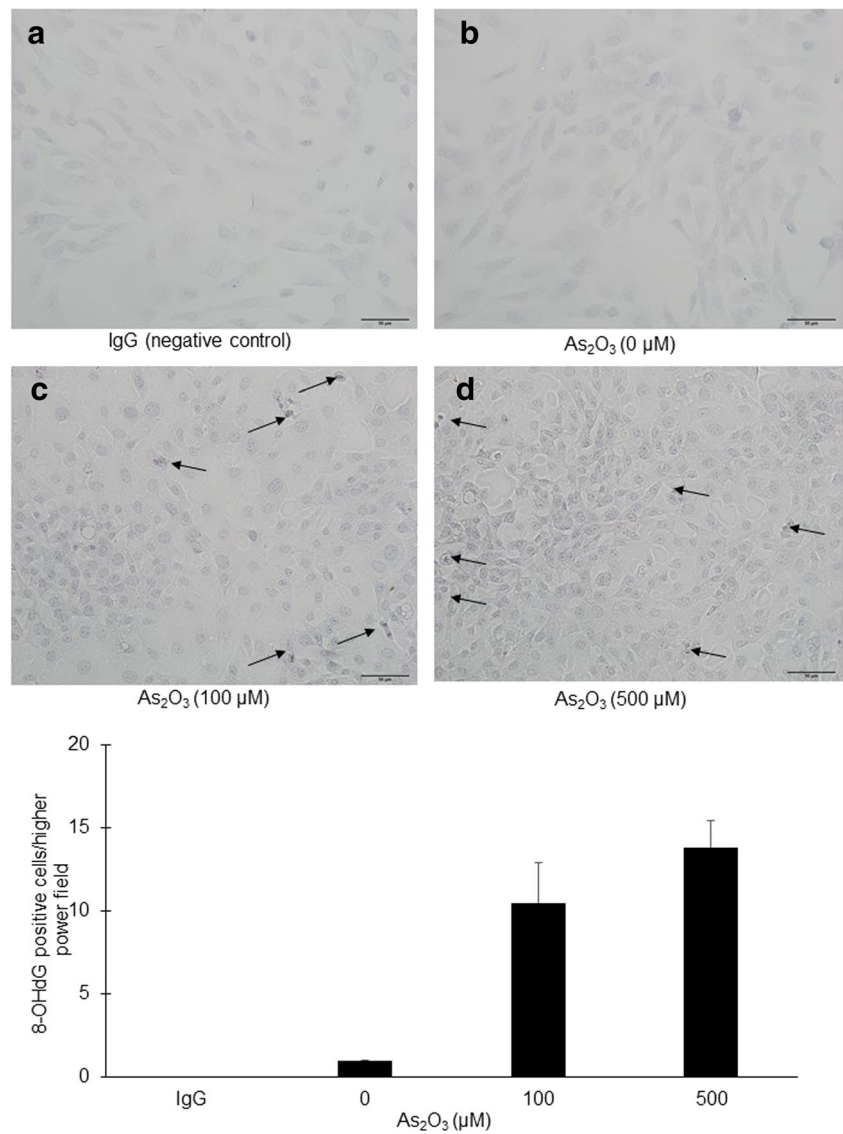
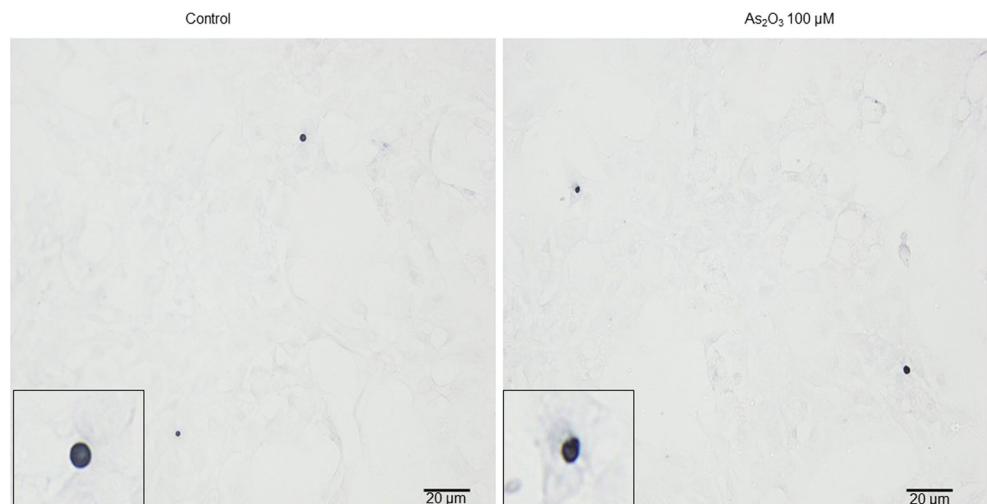


Fig. 4 Apoptosis assay by TUNEL staining. Cells treated with 100 μM As_2O_3 were analyzed for apoptosis by TUNEL procedure. Few TUNEL-positive cells (*black dots*) can be observed in both control and As_2O_3 -treated cells, with no significant difference between the two groups



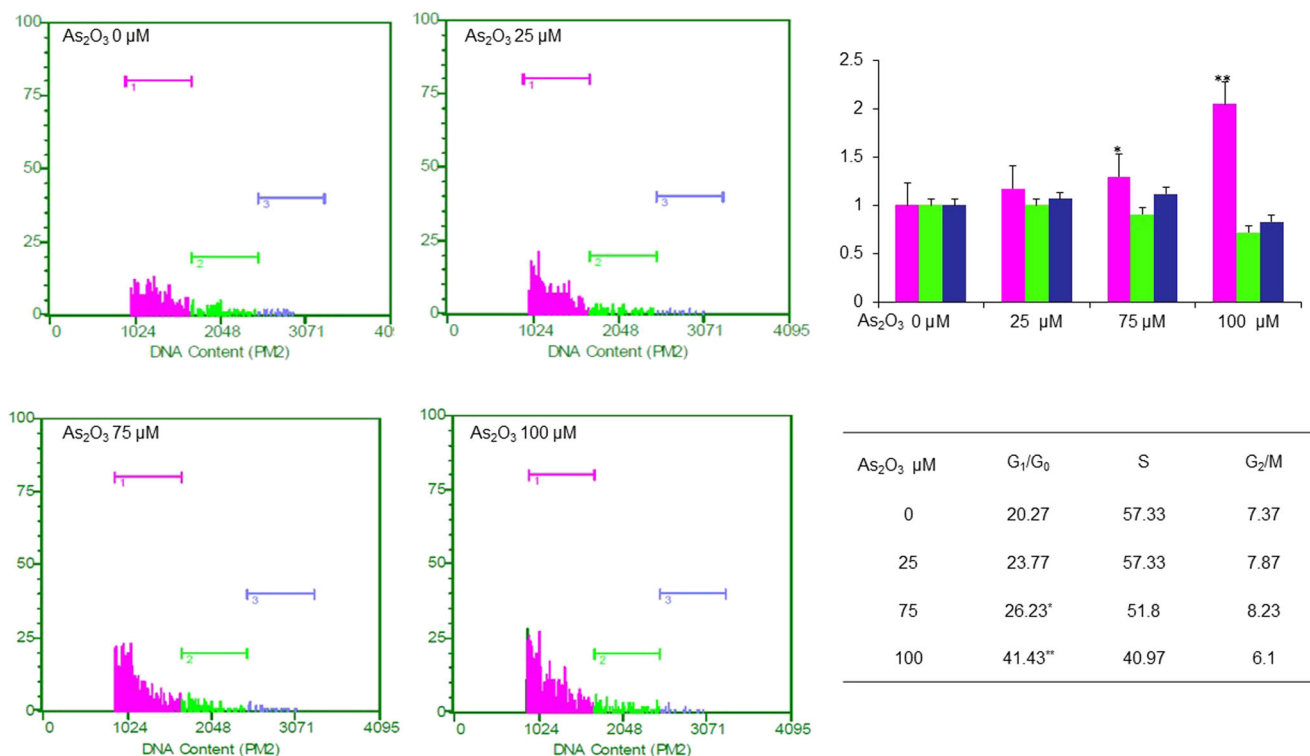


Fig. 5 Flow cytometry cell cycle analysis assay. Cells treated with different concentrations of As₂O₃ (0, 25, 75, and 100 μM) were analyzed for cell cycle populations. Treatment with higher concentrations of As₂O₃ caused an increase in number of cells in the

G₁/G₀ phase (histogram; pink: G₁/G₀, green: S, blue: G₂/M). Values are presented as mean ± SEM from three independent experiments. Double asterisks indicate *p* < 0.05 vs control groups

of positive cells vs As₂O₃ concentration. A total of nine slides per condition from three independent experiments were counted.

Cell cycle analysis by flow cytometry

Cells were seeded in six-well plates at a density of 3 × 10⁵ cells/well. Following incubation with different concentrations of As₂O₃ (0, 25, 50, 100 μM) for 18 h, the cells were fixed with 70% cold ethanol for 1 h at -20 °C and stained with Guava® cell cycle reagent (Merck Millipore, Darmstadt, Germany) according to the manufacturer’s instructions. Flow cytometry analysis was performed using Guava EasyCyte Mine (Millipore, Hayward CA, USA). The flow cytometer running conditions were set as follows: refresh rate was set to 1000 events/sample with a very slow flow rate of 0.1 μL/s. FSC gain setting was fixed to count 10,000 cells. Flow cytometry data were analyzed using Cyto Soft version 4.2 (Millipore). Data shown is a representative of three independent experiments; each experiment was performed in triplicate.

Statistical analysis

Results were expressed as mean ± standard deviation of control and treated cells from three independent experiments.

Nine replicates were first subjected to basic distributive statistics to judge the pattern of normal distribution. After judging the distribution pattern, further statistical analysis was carried out using non-parametric test using the Kruskal-Wallis test because the median and interquartile ranges of the variable showed an even distribution. Statistical significant analysis was done using post hoc Mann-Whitney test. *p* < 0.05 was set as the significant level between each group.

Results and discussion

Preliminary studies employing LDH and MTT assays showed that As₂O₃ was not cytotoxic and did not affect the viability of fibroblast cells, at any dose tested (data not shown). Next, it was tested if As₂O₃ could contribute to the generation of intracellular ROS in normal fibroblast cells, since studies on cancer cells reveal that arsenic mediated the generation of ROS in leukemia cells (Yedjou and Tchouwou 2007) and oxidative stress-induced DNA damage in hepatocellular carcinoma cells (Alarifi et al. 2013). Results obtained indicated that As₂O₃ induced generation of intracellular ROS in a dose-dependent manner (Fig. 1). The rate of ROS production among groups was statistically significant against the non-treated group; however, 100 and 500 μM showed no statistical

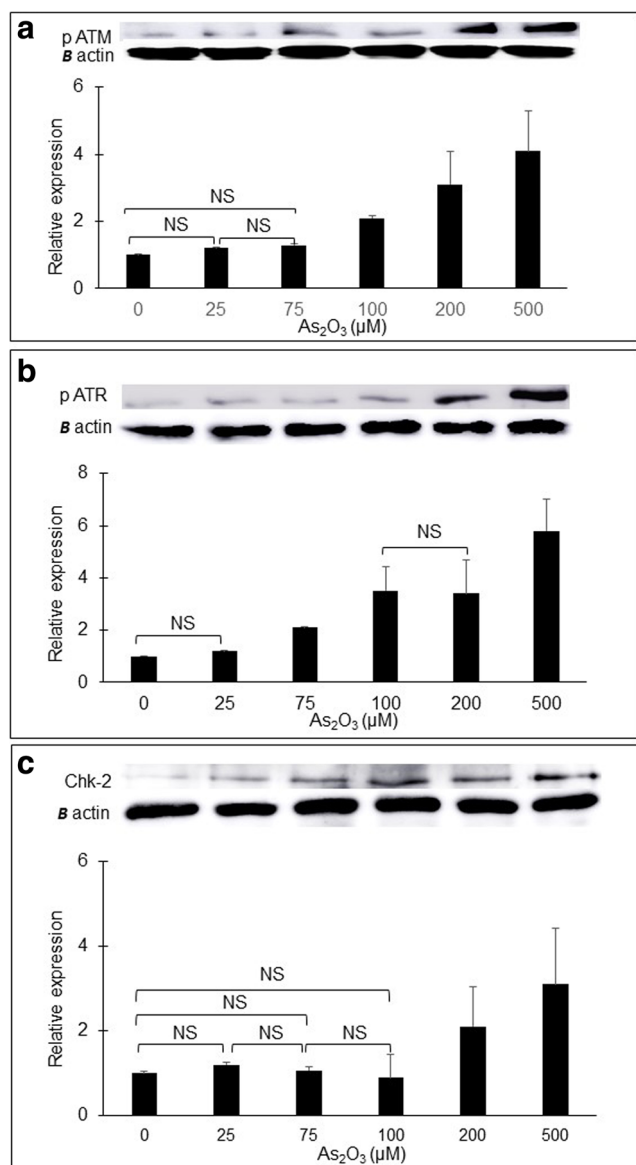


Fig. 6 W.B. analysis. Protein expression patterns of pATM, pATR, and Chk2 in different concentrations (0, 25, 75, 100, 200, and 500 μM) of As_2O_3 -treated cells. β -Actin was used as loading control. Treatment with higher concentrations of As_2O_3 caused an increase in expressions of pATM (a), pATR (b), and Chk2 (c) proteins. Non-significant (NS) groups were marked. Non-marked groups showed significant ($p < 0.05$) difference as analyzed by the Kruskal-Wallis test. Values are representatives of mean \pm SEM from three independent experiments

significance. Intracellular ROS generation was also confirmed by the immunofluorescence technique. Cells treated with 100 μM As_2O_3 showed a significant increase in the number of fluorescent cells, indicating increased ROS generation (Fig. 2). The interaction of reactive oxygen species with the DNA molecule can oxidise the nucleoside 2'-deoxyguanosine, leading to the synthesis of 8-hydroxy deoxyguanosine (8-OHdG), one of the most important markers for measuring

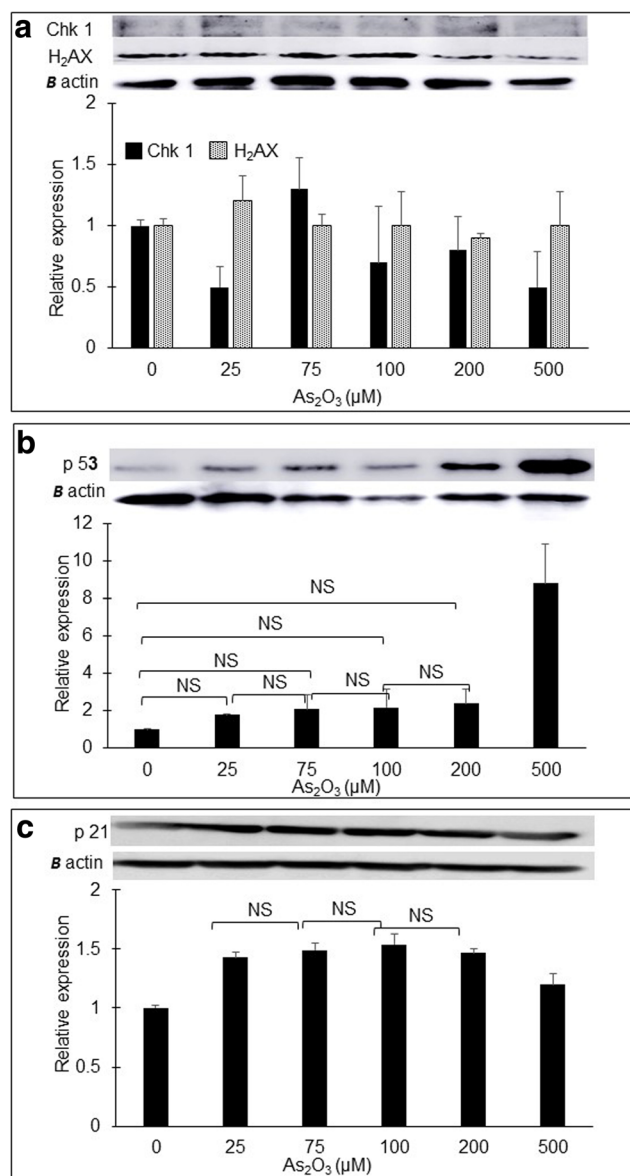
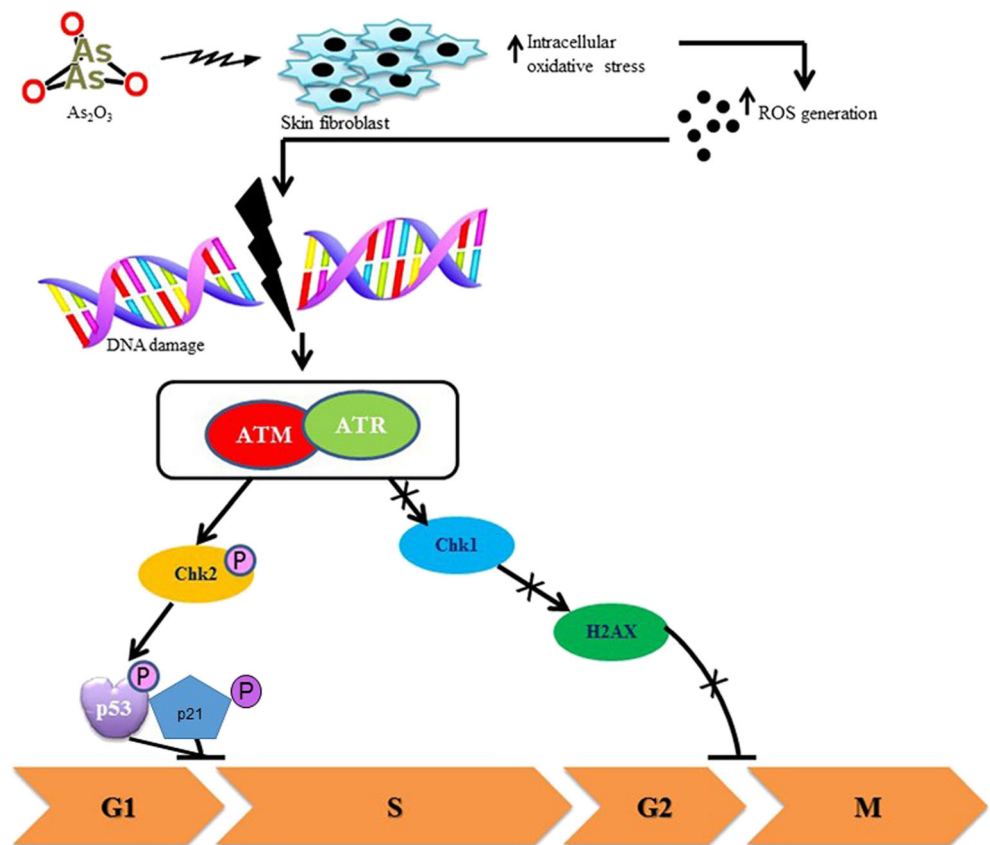


Fig. 7 W.B. analysis. Western blotting of Chk1, H2AX, p53, and p21. Relative expressions of Chk1, H2AX, p53, and p21 proteins in As_2O_3 -treated cells are plotted. β -Actin was used as loading control. Treatment with higher concentrations of As_2O_3 did not affect expression of Chk1 and H2AX (a), but caused an increase in expressions of p53 (b) and p21 (c) proteins. Non-significant (NS) groups were marked. Non-marked groups showed significant ($p < 0.05$) difference as analyzed by the Kruskal-Wallis test. Values are representatives of mean \pm SEM from three independent experiments

endogenous oxidative damage to DNA (Valavanidis et al. 2009). Furthermore, immunohistochemistry analysis revealed a dose-dependent increase in the number of 8-OHdG-positive cells, in As_2O_3 -treated groups in comparison to control groups (Fig. 3), indicating that As_2O_3 caused a build-up of oxidative stress in the fibroblast cells. Oxidative stress is an important contributor to diseases, through its effect on DNA (Dizdaroğlu 1992). Experimental evidences reveal that arsenic can cause cell damage and death through ROS signaling (Gao et al.

Fig. 8 Schematic representation of arsenic-induced cell cycle arrest in dermal fibroblast cells. Exposure of dermal fibroblast cells to As_2O_3 results in ROS-mediated DNA damage, activating the ATM/ATR kinase signaling cascades. ATM phosphorylates the checkpoint effector kinase Chk-2, which can prevent replication of damaged DNA by activating p53, resulting in G1/S checkpoint arrest



2004). Cells respond to DNA damage either by halting cell cycle progression or by undergoing apoptosis (Kastan and Bartek 2004). Preliminary studies showed that As_2O_3 did not induce cytotoxicity, reducing the possibility of inducing apoptosis. Nevertheless, the TUNEL assay was conducted to study apoptosis. Results obtained confirmed that As_2O_3 did not induce apoptosis in normal fibroblast cells (Fig. 4). On the other hand, flow cytometry analysis demonstrated that As_2O_3 treatment caused a significant percentage of cells to accumulate in the G0/G1 phase with a concomitant reduction in the S phase (Fig. 5). No significant differences were observed in the percentage of DNA count in the G2/M phase. The results throw light on the finding that As_2O_3 induced cell cycle arrest at the G0/G1 phase.

Arsenic inactivates a number of enzymes that are involved in cellular energy pathways, as well as DNA replication and repair (Ratnaik 2003). Cellular responses to DNA damage are coordinated primarily by kinase signaling cascade and the ATM-Chk2 and ATR-Chk1 pathways (Smith et al. 2010). Western blotting analysis revealed that As_2O_3 caused a dose-dependent increase in the expression levels of phosphorylated forms of ATM and ATR and total Chk2 (Fig. 6). In contrast, the protein expressions of Chk1 and H2AX were not affected by treatment with As_2O_3 (Fig. 7a). While Chk1 is a chromatin-associated protein that is phosphorylated by ATR (Stracker et al. 2009) and is the primary effector of intra-S and

G2/M phase checkpoints, Chk2 is a ubiquitous protein that is activated primarily by ATM (Ahn et al. 2004) and exerts a partial influence on the intra-S and G1/S checkpoints (Bartek and Lukas 2003). This study revealed an increase in the expressions of ATM, ATR, and Chk2 proteins, with a concomitant arrest of cell cycle at the G1 phase. As_2O_3 has been shown to induce G1 and/or G2-M phase arrest in myeloma cells (Liu et al. 2003), with simultaneous induction of the cyclin-dependent kinase inhibitor p21, which mediated p53-dependent cell cycle arrest (Liu et al. 2003). Exposure of normal fibroblasts to As_2O_3 resulted in increased expressions of p53 (Fig. 7b) and p21 (Fig. 7c). p53 is strongly activated by DNA damage and replication stress (Kruse and Gu 2009) and contributes significantly to numerous growth inhibitory pathways, including cell cycle checkpoints, apoptosis, and senescence (Vogelstein et al. 2000). ATM, ATR, Chk1, and Chk2 have all been reported to directly phosphorylate p53 (Hirao et al. 2002). ATM activates Chk2 by phosphorylation (Melchionna et al. 2000), and Chk2 in turn phosphorylates p53 (Shieh et al. 2000), thus stabilizing it. p53 functions as a tumor suppressor through its effect on apoptosis (Jiang et al. 2001). However, this study failed to witness any evidence of apoptosis induced by As_2O_3 ; the probable cause could lie with the increased expression of p21, a multi-functional protein that is responsible for the fine-tuned balance between cell cycle arrest/repair/ survival, apoptosis, and senescence/quiescence

(Kreis et al. 2015). Overexpression of p53 or p21 has been shown to cause premature senescence-related cell cycle arrest in low passage fibroblasts. On the one hand, p53-dependent increase in p21 expression suppresses cyclin-associated cdk2 activities, thereby preventing G1 to S phase progression (Woods and Vousden 2001). On the other hand, increased p21 localizes in the cytoplasm and blocks apoptosis, facilitating possibly the induction of senescence and metastasis. Senescence induced by p21 was anticipated to function as a tumor suppressor. However, recent studies reveal that senescent cells secrete factors like interleukins or matrix metalloproteinases, which function to promote tissue repair and tumor progression (Romanov et al. 2012), and senescence could also alter the cellular DNA scission (Madhyastha and Vatsala 2010). p21 is reported to be involved in inhibition of apoptosis through binding with a number of pro-apoptotic proteins to inactivate them. By inhibiting apoptosis, p21 is believed to contribute to carcinogenesis. The present study provides evidence that exposure of normal fibroblast cells to As₂O₃ could induce DNA damage through oxidative stress, stall regular cell cycle progression, and activate oncogene proteins such as p21 (Fig. 8). Although more in-depth analysis is required to clarify the mechanism of the As₂O₃-p21 interaction in inducing carcinogenesis in normal cells, the current findings help to contribute towards a better understanding of the pathological effects of As₂O₃ on normal fibroblast cells.

Compliance with ethical standards

Conflict of interest The authors declare that they have no conflict of interest.

References

- Ahn J, Urist M, Prives C (2004) The Chk2 protein kinase. *DNA Repair (Amst)* 3:1039–1047
- Alarifi S, Ali D, Alkahtani S, Maqsood AS, Bahy AA (2013) Arsenic trioxide-mediated oxidative stress and genotoxicity in human hepatocellular carcinoma cells. *Onco Targets and Ther* 6:75–84
- Bartek J, Lukas J (2003) Chk1 and Chk2 kinases in checkpoint control and cancer. *Cancer Cell* 3:421–429
- Chen C, Chen C, Wu M, Kuo T (1992) Cancer potential in liver, lung, bladder and kidney due to ingested inorganic arsenic in drinking water. *Br J Cancer* 66:888–892
- Crow JP (1997) Dichlorodihydrofluorescein and dihydrorhodamine 123 are sensitive indicators of peroxynitrite in vitro: implications for intracellular measurement of reactive nitrogen and oxygen species. *Nitric Oxide* 1:145–157
- Dilda PJ, Hogg PJ (2007) Arsenical-based cancer drugs. *Cancer Treat Rev* 33:542–564
- Ding W, Hudson LG, Liu KJ (2005) Inorganic arsenic compounds cause oxidative damage to DNA and protein by inducing ROS and RNS generation in human keratinocytes. *Mol Cell Biochem* 279:105–112
- Dizdaroglu M (1992) Oxidative damage to DNA in mammalian chromatin. *Mutat Res* 275:331–342
- Gao F, Yi J, Yuan JQ, Shi GY, Tang XM (2004) The cell cycle related apoptotic susceptibility to arsenic trioxide is associated with the level of reactive oxygen species. *Cell Res* 14:81–85
- Gavrieli Y, Sherman Y, Ben-sasson SA (1992) Identification of programmed cell death in situ via specific labeling of nuclear DNA fragmentation. *J Cell Biol* 119:493–501
- Graham-Evans B, Tchounwou PB, Cohly HP (2003) Cytotoxicity and proliferation studies with arsenic in established human cell lines: keratinocytes, melanocytes, dendritic cells, dermal fibroblasts, microvascular endothelial cells, monocytes and T-cells. *Int J Mol Sci* 4:13–21
- Halliwell B (2000) Why and how should we measure oxidative DNA damage in nutritional studies? How far have we come? *Am J Clin Nutr* 72:1082–1087
- Hirao A, Cheung A, Duncan G, Girard PM, Elia AJ, Wakeham A, Okada H, Sarkissian T, Wong JA, Sakai T, De Stanchina E, Bristow RG, Suda T, Lowe SW, Jeggo PA, Elledge SJ, Mak TW (2002) Chk2 is a tumor suppressor that regulates apoptosis in both an ataxia telangiectasia mutated (ATM)-dependent and an ATM-independent manner. *Mol Cell Biol* 22(18):6521–6532
- Hishikawa Y, Tamaru N, Ejima K, Hayashi T, Koji T (2004) Expression of keratinocyte growth factor and its receptor in human breast cancer: its inhibitory role in the induction of apoptosis possibly through the overexpression of Bcl-2. *Arch Histol Cytol* 67:455–464
- International Agency for Research on Cancer (2004) Some drinking water disinfectants and contaminants, including arsenic. In: IARC Monographs on the evaluation of carcinogenic risks to human IARC monographs, WHO Press, 84 Geneva, Switzerland
- Jiang XH, Wong CY, Yuen ST, Jiang SH, Cho CH, Lai KC, Marie CM, Lin Kung HF, Lam SK (2001) Arsenic trioxide induces apoptosis in human gastric cancer cells through up-regulation of P53 and activation of caspase-3. *Int J Cancer* 91:173–179
- Kastan MB, Bartek J (2004) Cell-cycle checkpoint and cancer. *Nature* 423:316–323
- Kreis NN, Louwen F, Yuan J (2015) Less understood issues: p21^{Cip1} in mitosis and its therapeutical. *Oncogene* 43:1758–1767
- Kruse JP, Gu W (2009) Modes of p53 regulation. *Cell* 137:609–622
- Liu Q, Hilsenbeck S, Gazitt Y (2003) Arsenic trioxide-induced apoptosis in myeloma cells: p53-dependent G1 or G2/M cell cycle arrest, activation of caspase-8 or caspase-9, and synergy with APO2/TRAIL. *Blood* 101:4078–4087
- Madhyastha H, Vatsala TM (2010) Cysteine rich cyanopeptide beta 2 from *Spirulina fusciformis* exhibits plasmid DNA pBR322 scission prevention and cellular antioxidant activity. *Indian J Exp Biol* 48:486–493
- Madhyastha R, Madhyastha H, Nakajima Y, Omura S, Maruyama M (2010) Curcumin facilitates fibrinolysis and cellular migration during wound healing by modulating urokinase plasminogen activator expression. *Pathophysiol Haemost Thromb* 37:59–66
- Melchionna R, Chen XB, Blasina MGCH (2000) Threonine 68 is required for radiation-induced phosphorylation and activation of Cds1. *Nat Cell Biol* 2:762–765
- Mosmann T (1983) Rapid calorimetric assay for cellular growth and survival: application to proliferation and cytotoxicity assays. *J Immunol Methods* 65:55–63
- Ratnaik RN (2003) Acute and chronic arsenic toxicity. *Postgrad Med J* 79:391–396
- Reichard J, Puga A (2010) Effects of arsenic exposure on DNA methylation and epigenetic gene regulation. *Epigenomics* 1:87–104
- Romanov VS, Pospelov VA, Pospelova TV (2012) Cyclin-dependent kinase inhibitor p21^(Waf1): contemporary view on its role in senescence and oncogenesis. *Biochem Mosc* 77:575–584

- Shieh SY, Ahn J, Tamai K, Taya Y, Prives C (2000) The human homologs of checkpoint kinases Chk1 and Cds1 (Chk2) phosphorylate p53 at multiple DNA damage-inducible sites. *Genes Dev* 14:289–300
- Smith A, Smith M (2004) Arsenic drinking water regulations in developing countries with extensive exposure. *Toxicology* 198:39–44
- Smith J, Tho LM, Xu N, Gillespie DA (2010) The ATM-Chk2 and ATR-Chk1 pathways in DNA damage signaling and cancer. *Cancer Res* 10:73–112
- Stracker TH, Usui T, Petrini JH (2009) Taking the time to make important decisions: the checkpoint effector kinases Chk1 and Chk2 and the DNA damage response. *DNA Repair (Amst)* 8:1047–1054
- Valavanidis A, Vlachogianni T, Fiotakis C (2009) 8-Hydroxy-2'-deoxyguanosine (8-OHdG): a critical biomarker of oxidative stress and carcinogenesis. *J Environ Sci Health C Environ Carcinog Ecotoxicol Rev* 27(2):120–139
- Vogelstein B, Lane D, Levine AJ (2000) Surfing the p53 network. *Nature* 408:307–310
- Woods DB, Vousden KH (2001) Regulation of p53 function. *Exp Cell Res* 264:56–66
- World Health Organization (2006) Guidelines for drinking-water quality. 1st addendum to 3rd Edn, Vol.1. Recommendation, Geneva
- Yamaguchi Y, Madhyastha H, Madhyastha R, Chojookhuu N, Hishikawa Y, Yutthana P, Nakajima Y, Maruyama M (2016) Arsenic acid inhibits proliferation of skin fibroblasts and increases cellular senescence through ROS mediated MST-1–FOXO signaling pathway. *J Toxicol Sci* 41:105–113
- Yedjou CG, Tchouwou PB (2007) In-vitro cytotoxic and genotoxic effects of arsenic trioxide on human leukemia (HL-60) cells using the MTT and alkaline single cell electrophoresis (comet) assays. *Mol Cell Biochem* 301:123–130
- You BR, Park WH (2012) Arsenic trioxide induces human pulmonary fibroblast cell death via increasing ROS levels and GSH depletion. *Oncol Rep* 28:749–757
- Yu H-S, Liao W-T, Yu C-YC (2006) Arsenic carcinogenesis in the skin. *J Biomed Sci* 13:657–666